

Preparation of ceramics pigment as nano-powder using organic fuels in approach for the solution combustion synthesis

A.El-Maghraby^{1,2} and Moamen S. Refat^{1,3}

¹Department of Chemistry, Faculty of Science, Taif University, Al-Haweiah, P.O. Box 888, Zip Code 21974, Taif, Saudi Arabia

² Ceramic Department, National Research Center, Tahrir Str., Dokki, Cairo, Egypt

³Department of Chemistry, Faculty of Science, Port Said University, Port Said, Egypt

Corresponding author: Prof. A.El-Maghraby

Abstract: The cobalt chromium aluminates spinel can be prepared by solid-state reactions which is opaque and has good hiding power is classified as ceramics grade pigment. The techniques have been applied to prepare ultrafine $\text{CoCrAl}_2\text{O}_4$ spinel as chemical combustion process, which has laid a good foundation for the development of the pigment-grade $\text{CoCrAl}_2\text{O}_4$ spinel characterized by a fine particle size and a uniform distribution. The crystalline powders have been synthesized by combustion process in a single step using a novel fuel urea and glucose. Urea and glucose as a fuel was used to prepare new nano size blue refractory ceramic pigments MgAl_2O_4 : as Co^{2+} and Cr^{3+} using low temperature combustion synthesis (LCS) method. The results can be prepared five batches at different percentage from Cr^{3+} to Al^{3+} and firing the batches at 700, 900, and 1100 °C. From the studies, the suitable temperature is at 900 C to form the crystal as spinel. The different percentage of Cr ion substitute Al ion in spinel lattice. The synthesized and calcite powders were characterized by Fourier transform infra red (FTIR) spectrometry, electronic spectra, thermogravimetry, differential thermogravimetry, differential thermal analysis, X-ray diffraction (XRD) analysis, and transmission electron microscopy (TEM). Also, the color measurements of nano pigments are studied by diffuse reflectance spectroscopy (DRS) using CIE-L*a*b* parameter method.

[A.El-Maghraby and Moamen S. Refat . **Preparation of ceramics pigment as nano-powder using organic fuels in approach for the solution combustion synthesis.** *Nat Sci* 2014;12(4):30-44]. (ISSN: 1545-0740). <http://www.sciencepub.net/nature>. 4

Keywords: ceramics pigment, nano-powder, organic fuels, combustion synthesis

1-Introduction

The magnesium aluminates, MgAl_2O_4 crystals present spinel structure, thus a lot of important properties used in industrial applications. The high melting point (2135 °C), the mechanical strength at high temperatures, chemical inertness and good thermal shock resistance are considerable properties which confer to the MgAl_2O_4 usability in the metallurgical, electrochemical, radiotechnical and chemical industrial fields [1–2]. Another inconvenient is the high number of operations (milling, mixing, consecutive firing), which can impurity the produced material. Many unconventional methods like: precipitation method,[3] the aerosol method,[4] the citrate–nitrate route,[5,6] classical sol–gel method[7,8] or modified sol–gel route by combining gelatin and coprecipitation processes[9] were used to produce MgAl_2O_4 spinel.

The spinel is a thermally and chemically stable pigment of intense color, which has been widely used for the coloration of plastics, paint, fibers, paper, rubber, phosphor, glass, cement, glazes, ceramic bodies and porcelain enamels [10].The spinel has been conventionally synthesized using solid state reactions which involve the mechanical mixing of various kinds of cobalt and aluminum or phosphate followed by a

calcinations at 1300 °C for a long period of time as well as an extended grinding. Solid-state reaction requires long-range diffusion of metal ions, which may result in homogeneity, larger and uneven grains (micron-sized) and poor control of stoichiometry. The unavoidable sintering caused by the high temperature calcinations leads to materials with a low surface area typically of the order of 1 to 5 m² g [10-11]. The cobalt aluminates or cobalt phosphate spinel by solid-state reactions which is opaque and has good hiding power is classified as ceramics grade pigment. Since 1980, wet-chemical techniques have been applied to prepare ultrafine CoAl_2O_4 and cobalt phosphate spinel such as chemical co-precipitation,[12-15] sol-gel [11,16] and polymeric precursor method [17], which has laid a good foundation for the development of the pigment-grade CoAl_2O_4 and cobalt phosphate spinel characterized by a fine particle size and a uniform distribution. The most attractive feature of the nano-sized pigment is the transparency effects it shows along with the color generation when dispersed in a matrix. Transparency and hiding power are two contrary characteristics of a pigment; the hiding power of transparent CoAl_2O_4 or cobalt phosphate spinel is 1/2–1/3 of that of a conventional one by solid-state reactions [12]. The special effect of transparency is

very popular in plastics, paints, etc. Furthermore, the Spinel by wet-chemical process has good control of stoichiometry, well-developed spinel-type structure and high purity which are in the interest of presenting a good tinting strength with a high degree of color saturation. The dispersity and dosage of the nano-sized pigment in the matrix is very important for getting a desired tinting effect and transparency.

The low temperature combustion synthesis (LCS) technique has been proved to be a novel, extremely facile, time-saving and energy-efficient route for the synthesis of ultrafine powders [18-22]. LCS is based on the gelling and subsequent combustion of an aqueous solution containing salts of the desired metals and some organic fuel, giving a voluminous and fluffy product with large surface area. In the present study, we report the synthesis of homogeneous nanocrystalline CoAl_2O_4 or cobalt phosphate pigments by LCS, an auto-ignited and self-sustaining combustion of citric acid-metal nitrates gel precursor.

The dehydrate belongs to the well-known series of isostructural crystallohydrates $\text{M}(\text{H}_2\text{PO}_4)_2 \cdot 2\text{H}_2\text{O}$ ($\text{M}=\text{Mg}, \text{Mn}, \text{Co}, \text{Ni}, \text{Fe}, \text{Zn}$), which have similar X-ray diffraction patterns and close unit cell parameters (they crystallize in monoclinic space group $\text{P}2_1/n$ with $Z = 2$) [21-27]. The $\text{M}(\text{H}_2\text{PO}_4)_2 \cdot 2\text{H}_2\text{O}$ was synthesized from metal(II) carbonate and phosphoric acid at low temperature (40-80 °C) with long time periods (> 8 h) [34, 35]. So far, only the crystal structure and thermal analysis of $\text{M}(\text{H}_2\text{PO}_4)_2 \cdot 2\text{H}_2\text{O}$ have been reported [28]. Most recently, Koleva et al. [29] reported the crystal structure and magnetic property of $\text{M}(\text{H}_2\text{PO}_4)_2 \cdot 2\text{H}_2\text{O}$ ($\text{M}=\text{Mg}, \text{Mn}, \text{Fe}, \text{Co}, \text{Ni}, \text{Zn}, \text{Cd}$). When calcite, dihydrogenphosphates yield cyclotetraphosphates, which are used as pigments, catalysts, and luminophore supporting matrices [9-12]. Therefore, thermal treatments of these dihydrogen phosphate hydrates have a great synthetic potential, which relates to the hydrate in the conventional crystal form. The presence of the water molecules influences the intermolecular interactions (affecting the internal energy and enthalpy) as well as the crystalline disorder (entropy) and, hence, influences the free energy, thermodynamic activity, solubility and stability, electrochemical and catalytic activity [30]. To control the state of hydration of the active ingredient, it is, therefore, important and necessary to understand the kinetics and mechanisms of decomposition and dehydration processes under the appropriate conditions. In many methods of kinetics estimation, conversional method is recommended as trustworthy way of obtaining reliable and consistent kinetic information [31]. It is a 'model-free method', which involves measuring the temperatures corresponding to fixed values of the extent of conversion (α) from experiments at different heating rates (β). The results obtained on

these bases can be directly applied in materials science for the preparation of various metals and alloys, ceramics, glasses, enamels, glazes, polymer and composite materials.

Combustion synthesis (CS) or self-propagating high-temperature synthesis (SHS) is an effective, low-cost method for production of various industrially useful materials. Today CS has become a very popular approach for preparation of nanomaterials and is practiced in 65 countries. Recently, a number of important breakthroughs in this field have been made, notably for development of new catalysts and nano-carriers with properties better than those for similar traditional materials. The extensive research carried out in last five years emphasized the SHS capabilities for materials improvement, energy saving and environmental protection. The importance of industrialization of the SHS process is also realized. All these aspects were adequately brought out and discussed in the international conference devoted to the 40th anniversary of SHS [32].

The developments in the combustion synthesis with special emphasis on the preparation of catalysts by solid state and solution combustion were discussed [32, 33]. It was concluded that the conventional solid state SHS being a gasless combustion process typically yield much coarser particles than solution combustion approach. One of the goals of this review is to discuss the various modifications made to conventional solid state SHS for preparing nanomaterials. Another important aim is to critically evaluate the recent progress and novel trends in solution combustion synthesis of nanomaterials as well as their application and scaling-up aspects. The review also focuses on the current status of studies on combustion synthesis of nanomaterials concentrating mainly on the publications, which have appeared in the last 1-year.

Thus the results on CS of nanomaterials are discussed using the processes classification that is based on the physical nature of the initial reaction medium:

- Conventional SHS of nanoscale materials, i.e. initial reactants are in solid state (condensed phase combustion).

- Solution-combustion synthesis (SCS) of nanosized powders, i.e. initial reaction medium is aqueous solution.

- Synthesis of nanoparticles in flame, i.e. gas-phase combustion.

Solution combustion synthesis (SCS) is a versatile, simple and rapid process, which allows effective synthesis of a variety of nanosize materials. This process involves a self-sustained reaction in homogeneous solution of different oxidizers (e.g., metal nitrates) and fuels (e.g., urea, glycine, hydrazides). Depending on the type of the precursors,

as well as on conditions used for the process organization, the SCS may occur as either volume or layer-by-layer propagating combustion modes. This process not only yields nanosize oxide materials but also allows uniform (homogeneous) doping of trace amounts of rare-earth impurity ions in a single step. Among the gamut of papers published in recent years on SCS, synthesis of luminescent materials and catalysts occupy the lion share. The latest developments in SCS technique are discussed based on the materials applications. The synthesis of nanophosphors is currently a hot topic in the field of CS [34–42].

It is well recognized that the fuel is an important component for the preparation of oxides by SCS. Urea and glycine are the most popular and attractive fuels for producing highly uniform, complex oxide ceramic powders with precisely controlled stoichiometry. The glycine nitrate process (GNP) has been billed as 'environmentally compatible'. But the recent study by Pine et al. has shown CO and NO_x as the products of incomplete combustion in GNP. Hence for GNP technique to be used on an industrial scale, the potential for producing and emitting hazardous nitrogen oxides and CO must be addressed seriously [43]. It is surprising to note that researchers worldwide have shown reluctance to use hydrazinebased fuels in recent years.

Use of different organic compounds such as: (i) alanine [44] (ii) asparagine, serine [45] (iii) methyl cellulose [46] (ii) ammonium acetate, ammonium citrate and ammonium tartarate have been explored as fuels [47]. After the publication of the first paper on the concept of mixture of fuels [48], large numbers of papers have been published on the use of combination of fuels such as citric and succinic acids [49]; citric acid and glycine [50], urea, monoethanolamine, alanine [51], etc. Although complex fuels favors formation of nanosize particles, in many cases a further calcinations is required to form organic free pure nanocrystalline powders. It is important to note that researchers are focusing their efforts towards the up scaling of SCS and also finding new applications of combustion synthesized nanosize powders.

Nano-pigments are inorganic or organic materials; insoluble, chemically and physically inert into the substrate or binders with particle size less than 100 nm [52, 53]. The ceramic pigments with particle size in the nano scale have massive potential market, because of their high surface area, which assures higher surface coverage, higher number reflectance points and hence improved scattering.

Ceramic pigments are basically a white or colored material, having high thermal stability and chemical resistance in order to be used at high temperature [54–56]. Recently the development of a new ceramic

pigment has fostered the research and application of pigments stable over 1200 °C. Ceramic pigments based on oxides, spinels, aluminates are prepared with blends of oxides as starting mixtures with proper particle size distribution of powders, also employing additions of salt like halides and borates that have mineralizing function [57,58]. Recently, attempts to synthesize ceramic materials at low temperatures have been carried out by several solution techniques such as sol-gel [59–62], co-precipitation [63], hydrothermal [64, 65], alkoxide hydrolysis [66–68], Penchini method [69, 70], and low combustion method [71–76]. White MgAl₂O₄ [77] and red Ce_{1-x}Pr_xO₂₋₁ [78] pigment powders are prepared by auto-ignition route (combustion method). Light or dark beige, brown and black ceramic powders Co_xZn_{7-x}Sb₂O₁₂ [79], light reddish-yellow ceramic pigment MgFe₂O₄ [80], brown pigment BaFe₂O₄ and red ceramic pigments CaFe₂O₄ [81, 82] were prepared using the polymeric precursor method. Co₂SiO₄ (olivine), (Co,Zn)₂SiO₄ (willemite), CoAl₂O₄ (spinel), Co₂SnO₄, (Co,Zn)Al₂O₄, Co(Al,Cr)₃O₄, (Co,Mg)Al₂O₄ and (Co,Zn)TiO₃ [83,84] are used as blue pigments. But cobalt is scarce and expensive, thus increasing the production costs of cobalt-based ceramic pigments. Moreover, serious environmental problems may occur from the manufacturing process of Co-based ceramic pigments [85, 86]. A new application of the spinels as ceramic pigments has been explored, owing to their high mechanical resistance, high thermal stability, low temperature sinterability and the easy incorporation of chromophore ions into the spinel lattice, allowing for different types of doping, thus producing ceramic pigments with different colors [87]. Blue pigments are widely used in industry to bring color to plastics, paints, fibers, papers, rubbers, glass, cement, glazes, ceramics, and porcelain enamels. The synthesis route is very important to determine the final properties of nano inorganic pigments such as coloring agent, particle size, resistance to acids and alkaline [88].

The aims at synthesizing ceramic blue green pigments from the system Co(Cr_xAl_{1-x})₂O₄ spinel nano ceramic pigments using low temperature combustion method using urea and glucose fuel. The Co (Cr_x Al_{1-x})₂O₄ system allows for a reduction in the production costs and also for minimizing the environmental damage, as the amount of cobalt is reduced.

2-Experimental

2.1. Raw materials

Analytical-grade Co (NO₃)₂·6H₂O, Al (NO₃)₃·9H₂O, urea (A.R) a glucose (A.R) were used as starting materials. The Cr (NO₃)₃·9H₂O prepared from CrCl₃·6H₂O and NaCO₃ in nitric acid see in Table 1.

Table 1: Materials used and characteristics

Materials	Formula	Company	purity
Cobalt nitrate	Co(NO ₃) ₃ .6H ₂ O	BDH Company	99.2 %
Aluminum nitrate	Al(NO ₃) ₃ .9H ₂ O	Fluka Company	99.3%
Chromium chloride	CrCl ₃ .6H ₂ O	BDH Company	99.8%
Sodium Carbonate	NaCO ₃	BDH Company	99.6
Urea	Co(NH ₂) ₂	Sigma Aldrich	98,6%
Glucose	C ₆ H ₁₂ O ₆	Sigma Aldrich	98,0%
Acetone	CH ₃ COCH ₃	BDH Company	99.0%

The experimental compositions are listed in Table 2, the mixing materials was them heated on hot drying with continuous agitation to evaporate gases after them from foaming.

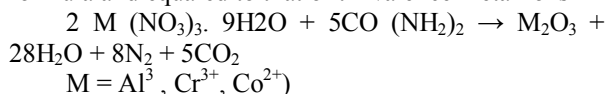
2.2. Preparation of Chromium nitrate

- Dissolve chromium chloride and sodium carbonate in water until to form solution to form chromium carbonate precipitation in solution
- Separation the chromium carbonate and washing the precipitate to remove all sodium chloride
- Added the nitric acid to the precipitate (chromium carbonate) and heat until 50 C to form crystal from chromium nitrate.

2.3. Synthesis of Co (Cr_x Al_{1-x}) O₄ nano pigments

Nano ceramics pigment Co (Cr_x Al_{1-x}) O₄ (0.1 ≤ x ≤ 0.5) were prepared using metal salt. The amount of

urea was according to the following chemical reaction formula and equaled to that of tri-valence metal ions



The amount of glucose was 20 wt% of the starting materials. Cr (NO₃)₃ 9H₂O, Al (NO₃)₃ 9H₂O, urea and glucose were mixed together. The starting materials were thoroughly milled until a blue green-like paste was formed and then the blue green like paste was fired at 100 °C, and black brown foaming forming powders were obtained. The foaming was milled until very fine powder. The black brown powder were finally fired by using muffle furnace at 700 °C ,900 °C 1100 °C , respectively, and the Co²⁺ , Cr³⁺ : Al³⁺ nano- powders with light black color were obtained.

Table 2: The Batches Composition of Co Al_{1-x} Cr_x O₄ Pigment Spinel

Batches	Co(NO ₃) ₃ .6H ₂ O	Cr(NO ₃) ₃ .9H ₂ O	Al(NO ₃) ₃ .9.H ₂ O	Urea	Glucose
Batch 1	20.52	4.89	41.26	20	13.3
Batch 2	20.43	9.73	36.50	20	13.3
Batch 3	20.33	14.54	31.79	20	13.3
Batch 4	20.24	19.29	27.13	20	13.3
Batch 5	20.15	24.01	22.51	20	13.3

2.4. Instruments

X-ray diffraction

X-ray diffraction (XRD) analysis was performed using an automated (Philips type: PW1840) diffractometer equipment with Cu K α radiation source and at a step size angle of 0.02 θ , scan rate of 2 θ in 2 θ unit, and a scan range from 10 θ to 60 θ .

Thermal analysis (DTA/TGA)

Differential thermal analysis (DTA) and thermogravimetric (TGA) were run with a coupled (SETARAM TG/DTA 92) DTA-TGA instrument. The batch was heated with rate of 5 C/min at ambient atmosphere pressure and temperature, up to 1000 °C.

Infrared Spectra

The infrared spectra of the reactants and the resulting samples were recorded in KBr discs on a Bruker IFS 113V FT-IR spectrometer, in the wave number range (4000–200 cm⁻¹).

Scanning electron microscopy

Morphology of the samples was determined by SEM. The samples were previously coated with gold. The samples were studied with a Philips®30 Analytical Scanning Electron Microscope. Particle images were obtained with a secondary electron detector.

Color measurement

The CIE $L^*a^*b^*$ colorimetric method, recommended by the Commission Internationale de l'Eclairage (CIE) was followed. In this method, L^* is lightness axis: black (0) – white (100), b^* is the blue (–) – yellow (+), a^* is the green (–) – red (+) axis.

3-Results and dissociation

3-1-Interpretation of parent adduct at room and high temperatures

The main purpose of this paper has been the study of the mode of decomposition of coordinated D-glucose/urea in presence of chromium(III)/cobalt(II) or

aluminum(III)/cobalt(II) complex systems in dry grinding at room and high temperatures. This enables us to compare between the procedures in literature and the present study which essential depend on the low cost materials. The reaction products obtained during the course of the reaction of D-glucose/urea with Cr(III)/Co(II) or Al(III)/Co(II) ions is shown to depend not only on the type of metal ion but also on the nature of the metal salt used in the reaction.

In previous studies many metal-urea complexes formed at room temperature have been isolated and characterized. In these complex systems, urea coordinates via either its oxygen or nitrogen atoms, depending on the type of metal ion. The present investigation was undertaken to study the nature of the reaction of urea with metal ions at room temperature. Furthermore, the role played by certain metal ions such as Cr^{3+} , Al^{3+} , and Co^{2+} on the decomposition of coordinated urea and D-glucose is of considerable interest. In recent years the chemistry of urea and related compound have attracted considerable interest and growing importance owing to the fact that some of these compounds are used as precursors [89-91].

Yamaguchi et al. [92] calculated the normal vibrations of the C_{2v} model of urea molecule as an eight-body problem using a potential function of the Urey-Bradley force field and obtained the force constants which have been refined by the least-squares method. Based on the result of these calculations, Yamaguchi [92] assigned all of the observed frequencies in the spectra of urea and urea- d_4 . To the two vibrations of the frequencies 1686 and 1603 cm^{-1} , there are considerable contributions of both CO stretching and NH_2 bending motions, whereas Stewart [93] assigned the 1686 cm^{-1} band to CO stretching vibration and the 1603 cm^{-1} band to NH_2 bending motion. The calculations studied by Yamaguchi showed that for the band at 1686 cm^{-1} , the contribution of the NH_2 bending motion is greater than that of CO stretching motion. The band at 1629 cm^{-1} corresponds

to almost pure NH_2 bending vibration. The NH_2 bending motion of A_1 type is equal to that of B_2 type. The A_1 type band should have a frequency of about 1630 cm^{-1} , if there is no coupling between NH_2 bending and CO stretching motions. On the other hand, the observed frequency of 1610 cm^{-1} of urea- d_4 is assigned to almost pure skeletal vibration. Therefore, the interaction between the 1630 and 1610 cm^{-1} vibration gives rise to the two observed bands at 1686 and 1603 cm^{-1} . The infrared bands of urea- d_4 observed at 1245 and 1154 cm^{-1} are assigned, respectively, to A_1 type and B_2 type, ND_2 bending vibrations. This assignment is consistent with the observed depolarization degrees of the Raman lines. The large frequency difference between the A_1 and B_2 vibrations is due to the fact that in the A_1 vibration, the cross term related to the CN stretching vibration is large. The 1464 cm^{-1} frequency of urea is assigned to the CN stretching vibration of B_2 type. The corresponding frequency of urea- d_4 is observed at 1490 cm^{-1} . The 1150 cm^{-1} band is assigned to NH_2 rocking vibrations of both A_1 and B_2 types. The normal vibration calculation yields almost the same values for these frequencies.

Urea possesses two types of potential donor atoms, the carbonyl oxygen and amide nitrogens. Penland et al. [94] studied the infrared spectra of urea complexes to determine whether coordination occurs through oxygen or nitrogen atoms. If urea coordinated through oxygen, this may result in a decrease of the CO stretching frequency but no appreciable change in NH stretching frequency. Since the vibrational spectrum of urea itself has been analyzed completely [93], band shifts caused by coordination can be checked immediately. Table (3) illustrates the effect of the coordination on the spectra of the parent adducts of urea and D-glucose with Cr (III)/Co (II) and Al (III)/Co (II) in which the coordination occurs through oxygen atom of urea and also, the D-glucose binding as a bidentate chelate through oxygen atoms of hydroxyl groups attached with C_7 and C_9 , respectively [94, 95].

Table 3: Infrared spectra of distinguish bands for the urea, D-glucose and parent adducts

Frequencies (cm^{-1})			
Urea	D-Glucose	Parent adduct	Assignments
3450, 3350	3411, 3311	3459, 3355, 3220	$\nu(\text{NH}_2)$; urea + $\nu(\text{O-H})$; D-glucose
1683	--	1634	$\nu(\text{C=O})$
1471	1460, 1376, 1347	1578, 1299	$\nu(\text{C-N})$; urea + $\nu(\text{C-O})$; D-glucose

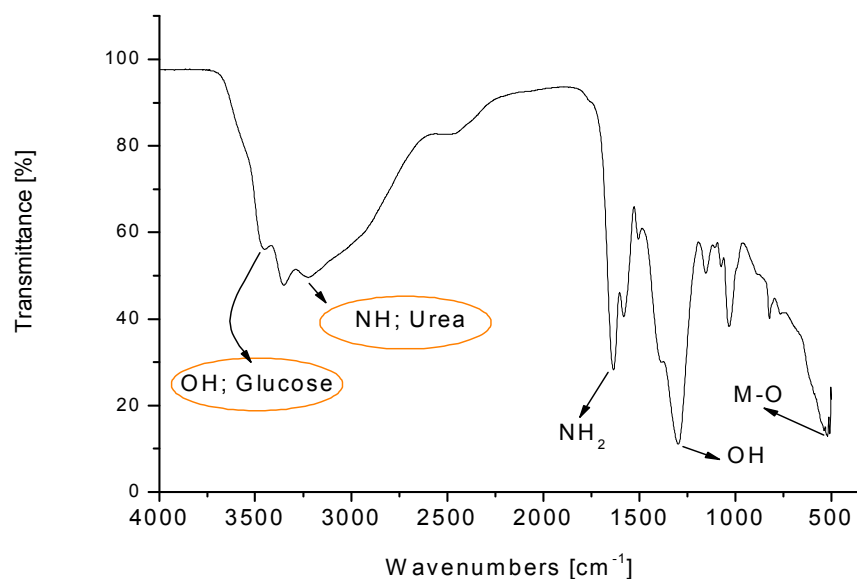


Fig. 1: Infrared spectra of urea/D-glucose with Cr (III)/Co (II) and Al (III)/Co (II) parent adducts

The infrared spectra of both parent adducts of urea and D-glucose with Cr(III)/Co(II) and Al(III)/Co(II) (Fig. 2, Table 3) and they indicated that, oxygen-to-metal bonds are present in these adducts. The infrared bands observed at 3450 and 3350 cm^{-1} in the spectrum of free urea are assigned to the N-H stretching vibrations. They are observed at almost the same frequencies in the spectra of both parent adducts prepared at room temperature (Fig. 2). The bands observed at about 1640 cm^{-1} in the spectra of the Cr (III)/Co (II) and Al (III)/Co (II) parent adducts are assigned to the NH_2 bending vibrations while the corresponding NH_2 rocking vibrations are observed at 1175 and 1170 cm^{-1} . However, the formation of the oxygen to metal bond in adducts increases the single bond character of the CO group and therefore, the $\nu(\text{CO})$ in these adducts are expected to occur at a lower frequency values compared with those of the free urea. The infrared spectra of both parent adducts Cr(III)/Co(II) and Al(III)/Co(II), Fig. 2, shows an extra set of bands compared with the starting materials, these bands exist at 1381, 886 cm^{-1} with very medium intensities and they are characteristic for the coordinated nitrate group, NO_3^- [95, 96]. The infrared spectra of urea/D-glucose with Cr (III)/Co (II) and Al (III)/Co (II) adducts are different from the spectra of both starting materials of glucose and urea. This differentiation reveals the presence of $\text{O} \rightarrow \text{M}$ coordinate bonds in the Cr (III)/Co (II) and Al (III)/Co (II) adducts. The majority of the evidences suggest that, the oxygen atom of urea and the oxygen atoms of hydroxyl groups of D-glucose at carbons C_7 and C_9 are

the preferred coordination site in most of the cases studied. A shift in the carbonyl and hydroxyl stretching frequency to lower value is usually taken to indicate the formation of a metal-oxygen linkage [97-100]. Infrared bands, the binding site for Cr (III)/Co (II) or Al (III)/Co (II) in the glucose ligand were identified as most likely the $\text{C}_7\text{-OH}$ and the $\text{C}_9\text{-OH}$. A negative shift of O-H (D-glucose) and C=O (urea) bond on coordination is probably due to drain of electrons towards oxygen as shown in structures (Figs. 3 and 4).

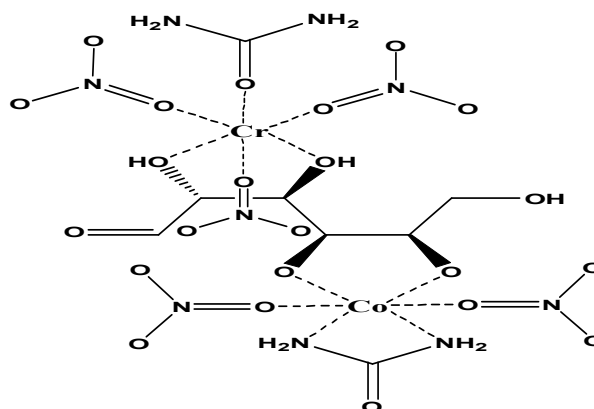


Fig. 2: Speculated structure of urea/D-glucose with Cr (III)/Co (II) parent adduct

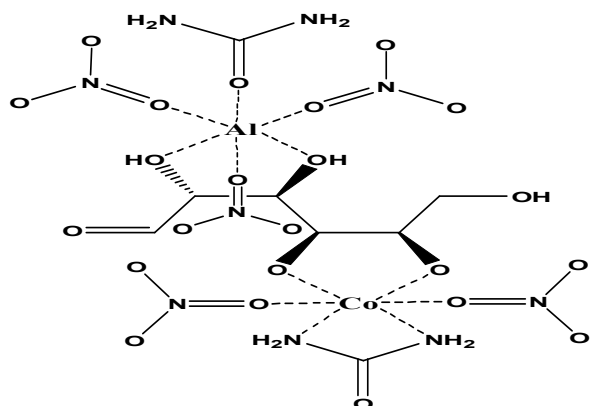
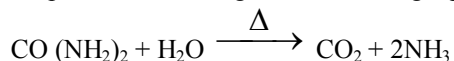


Fig. 3: Speculated structure of urea/D-glucose with Al (III)/Co (II) parent adduct

Free urea ($\text{CO}(\text{NH}_2)_2$) is known to decompose at high temperature according to the following equation;

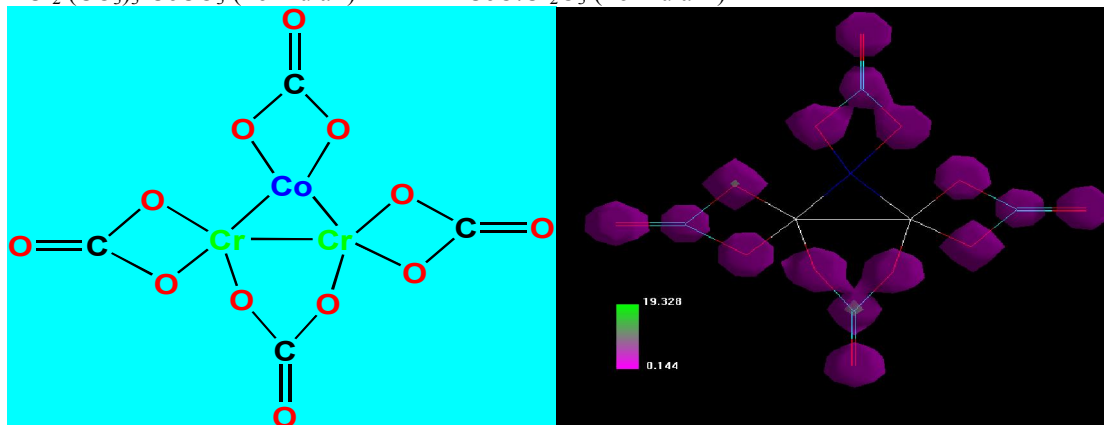
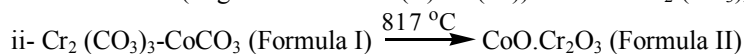
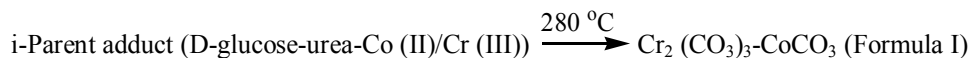


However, the coordinated urea in its complexes with metal ions seems to have different modes of decomposition. In previously studies [101, 102] the nature of decomposition of coordinated urea at high temperature and the role played by metal ions on this process. They concluded that, the decomposition of coordinated urea depends upon the type of metal ion as well as on the nature of the metal salt used in the reaction. The infrared spectra of the second adducts which collected after the heating of urea/D-glucose with Cr(III)/Co(II) and Al(III)/Co(II) first parent adducts at different temperatures (700, 900 and 1100 °C) are shown in Fig. 5. The infrared spectra of the final thermal decomposition products of these two adduct are shown in Fig. 6. The infrared spectra obtained for the two Cr(III)/Co(II) and Al(III)/Co(II)

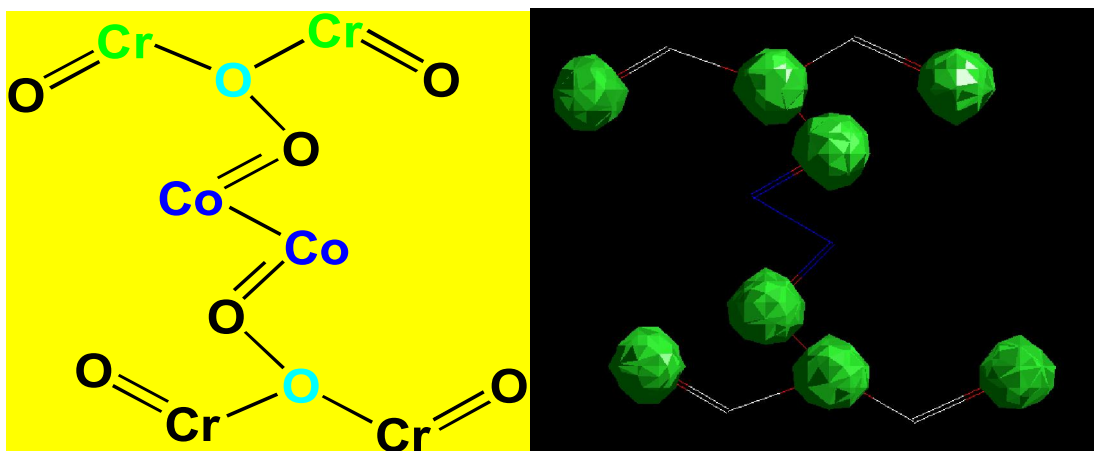
systems clearly show features in common, (i)-The absence of bands due to coordinated urea and D-glucose, (ii) The presence of a characteristic bands observed at about $\sim 1400 \text{ cm}^{-1}$ related to the bond vibrations, $\nu(\text{C-O})$ of CO_3^{2-} group [102], (iii) A set of bands attributed to the stretching vibrations of $\text{O} \rightarrow \text{M}$ bonds.

To establish the proposed formula and structures for each of the Cr (III)/Co (II) and Al (III)/Co (II) systems under investigation, thermogravimetric (TG/DTG) and differential thermal analysis (DTA) were carried and shown in Fig. 7. The data obtained support the proposed structures of the two systems and indicate the following;

The thermal degradation of the Cr (III)/Co (II) and Al (III)/Co (II) systems ignited previously at $\sim 300 \text{ }^\circ\text{C}$ take place in three degradation stages. These stages of decomposition occur at a maximum temperature of 123, 280 and 817 °C. The infrared spectrum of the thermal product at these temperature, Figs. 5 and 6, clearly indicate the formation of the CO_3^{2-} group with its characteristic $\nu(\text{C-O})$ at 1400 cm^{-1} [101, 102] resulted from the decomposition of urea and glucose at high temperature [103]. This important result strongly supports our conclusion concerning the structures of these systems under investigation. These stages of degradation at 179 °C are accompanied by weight of loss 5.00% corresponding to the loss of carbon dioxide molecules. The mass losses of these steps are independent from the heating rate. The mass loss of the second thermal decomposition step of glucose or urea, however, is strongly dependent on the heating rate. This is sufficient proof that after the first step the later decomposition follows at least two competing reaction paths represented in Formulas I and II.



Formula I: 3D and formula structure of $\text{Cr}_2(\text{CO}_3)_3\text{-CoCO}_3$



Formula II: 3D and formula structure of $\text{CoO} \cdot \text{Cr}_2\text{O}_3$

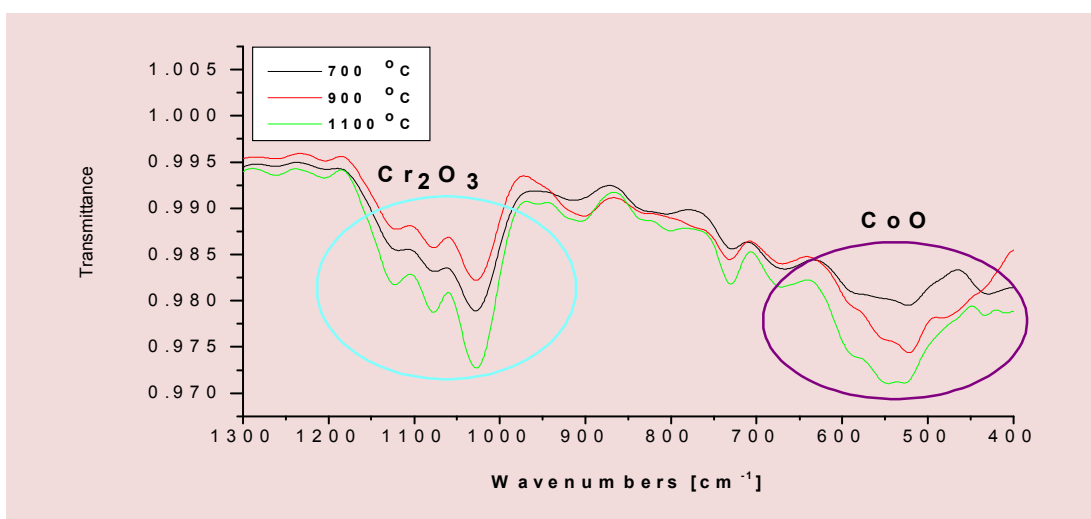


Fig. 4: Infrared spectra of urea/D-glucose with Cr(III)/Co(II) and Al(III)/Co(II) systems at different temperatures

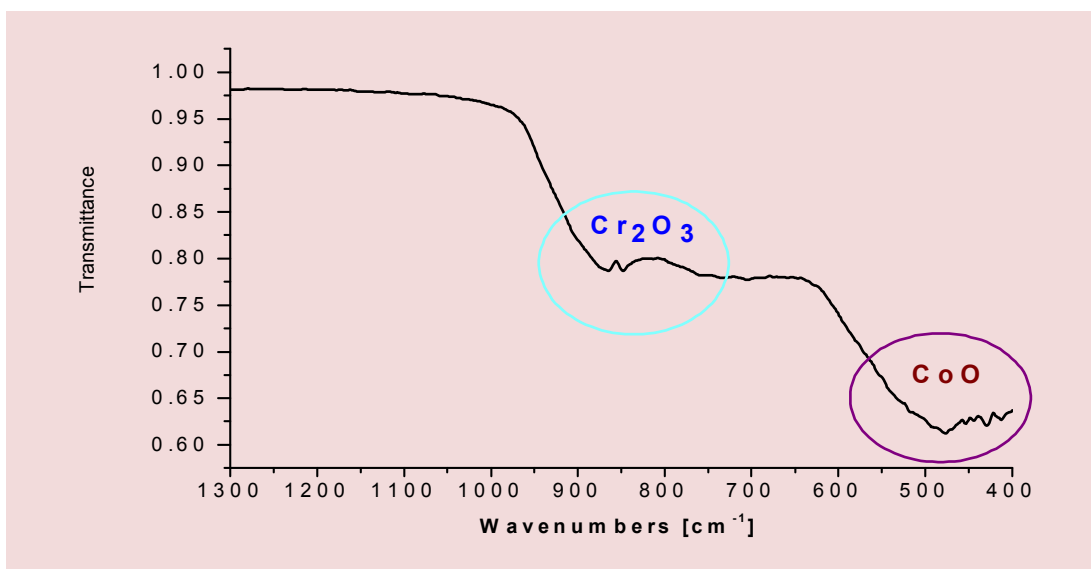


Fig. 5: Infrared spectra of residual products of urea/D-glucose with Cr(III)/Co(II) and Al(III)/Co(II) systems

Most commonly used methods are the differential method of Freeman and Carroll [104] integral method of Coat and Redfern [105] and the approximation method of Horowitz and Metzger [106]. In the present investigation, the general thermal behaviors of the Cr (III)/Co (II) and Al (III)/Co (II) systems ignited previously at ~ 300 °C in terms of stability ranges, peak temperatures and values of kinetic parameters are discussed. The kinetic parameters have been evaluated using the Coats-Redfern equation:

$$\int_0^\alpha \frac{d\alpha}{(1-\alpha)^n} = \frac{A}{\varphi} \int_{T_1}^{T_2} \exp\left(-\frac{E^*}{RT}\right) dt \quad (1)$$

This equation on integration gives;

$$\ln\left[-\frac{\ln(1-\alpha)}{T^2}\right] = -\frac{E^*}{RT} + \ln\left[\frac{AR}{\varphi E^*}\right] \quad (2)$$

Where φ is the linear heating rate, R is the gas constant, T is the DTG temperature peak, α , is the fraction of the sample decomposed at time t , A is the pre-exponential factor. A plot of left-hand side against

$1/T$ was drawn. E^* is the energy of activation in J mol^{-1} and calculated from the slop and A in (s^{-1}) from the intercept value. The entropy of activation ΔS^* in ($\text{JK}^{-1} \text{mol}^{-1}$) was calculated by using the equation:

$$\Delta S^* = R \ln(Ah/k_B T_s) \quad (3)$$

Where k_B is the Boltzmann constant, h is the Plank's constant and T_s is the DTG peak temperature [19].

The Horowitz-Metzger equation is an illustrative of the approximation methods.

$$\log\left[\frac{1-(1-\alpha)^{1-n}}{(1-\alpha)}\right] = E^* \theta / 2.303RT_s^2 \text{ for } n \neq 1 \quad (4)$$

When $n = 1$, the LHS of equation 4 would be $\log[-\log(1-\alpha)]$. For a first-order kinetic process the Horowitz-Metzger equation may be written in the form:

$$\text{Log}[\log(w_\alpha / w_\gamma)] = E^* \theta / 2.303RT_s^2 - \log 2.303$$

Where $\theta = T - T_s$, $w_\gamma = w_\alpha - w$, $w_\alpha =$ mass loss at the completion of the reaction. The plot of $\log[\log(w_\alpha / w_\gamma)]$ vs. θ was drawn and found to be linear from the slope of which E^* was calculated. The pre-exponential factor, A , was calculated from the equation:

$$E^* / RT_s^2 = A / [\varphi \exp(-E^* / RT_s)]$$

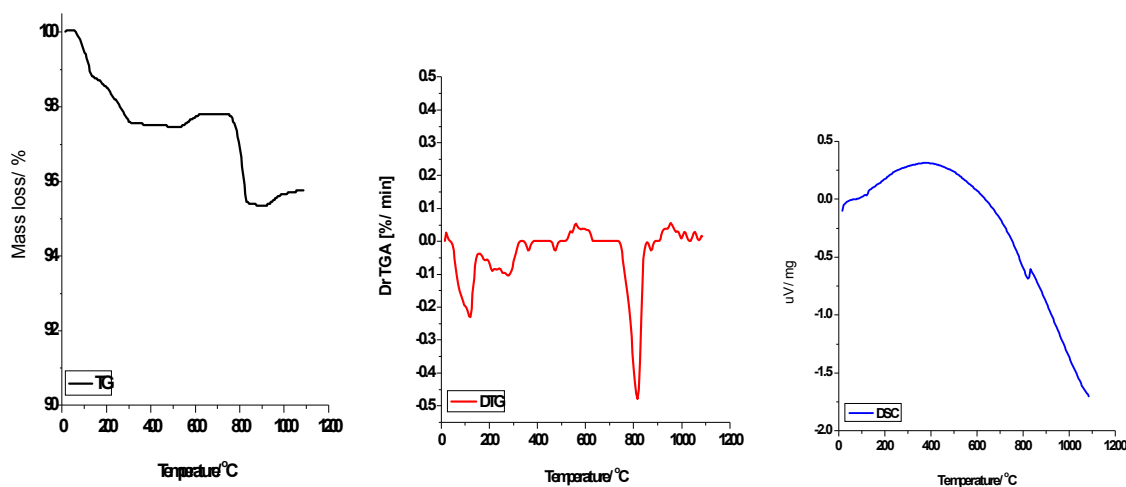


Fig. 6: TG, DTG and DSC curves of Cr (III)/Co (II) system ignited previously at 300 °C

Table 4: Kinetic parameters of Cr (III)/Co (II) system

Method	Parameter					
	E / kJmol^{-1}	Z / s^{-1}	$\Delta S / \text{Jmol}^{-1}\text{K}^{-1}$	$\Delta H / \text{kJmol}^{-1}$	$\Delta G / \text{kJmol}^{-1}$	r
HM	165	11.00×10^{12}	42	162	141	0.9953
CR	170	12.21×10^{14}	44	159	146	0.9943

The entropy of activation, ΔS^* , was calculated from equation 3. The enthalpy activation, ΔH^* , and Gibbs free energy, ΔG^* , were calculated from; $\Delta H^* = E^* - RT$ and $\Delta G^* = \Delta H^* - T\Delta S^*$, respectively. In the present investigation, the general thermal behaviors of the Cr (III)/Co (II) and Al (III)/Co (II) systems in terms of stability ranges, maximum temperature peaks and

values of kinetic parameters, are shown in Table (4) and Fig. 8. The kinetic and thermodynamic parameters are evaluated using the Coats-Redfern and Horowitz-Metzger equations [105, 107]. The entropy of activation, ΔS^* , is calculated. The enthalpy activation, ΔH^* , and Gibbs free energy, ΔG^* , are calculated from $\Delta H^* = E^* - RT$ and $\Delta G^* = \Delta H^* - T\Delta S^*$, respectively.

The thermodynamic behavior is non-spontaneous (more ordered) reactions (ΔS is negative value), endothermic reactions ($\Delta H > 0$) and endergonic ($\Delta G > 0$), during the reactions. The thermodynamic data obtained with the two methods are in harmony with each other. The correlation coefficients of the Arrhenius plots of the thermal decomposition steps were found to lie in the range ~ 0.99 , showing a good

fit with linear function. The thermograms and the calculated thermal parameters for the systems show that the stability of these adducts depends on the nature of the central metal ion. The thermal stability of the metal complexes was found to increase periodically with increase in atomic number of the metal and the larger value of charge/radius ratio [108,109].

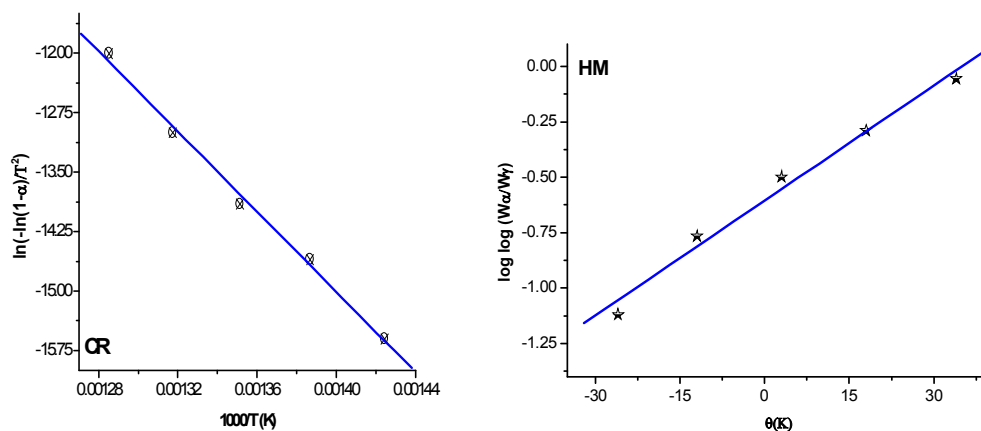


Fig. 7: Kinetic curves of Cr (III)/Co (II) and Al (III)/Co (II) systems ignited previously at 300 °C using Coat and Redfern (CR) and Horowitz and Metzger (HM) methods

3.3. XRD analysis of the samples

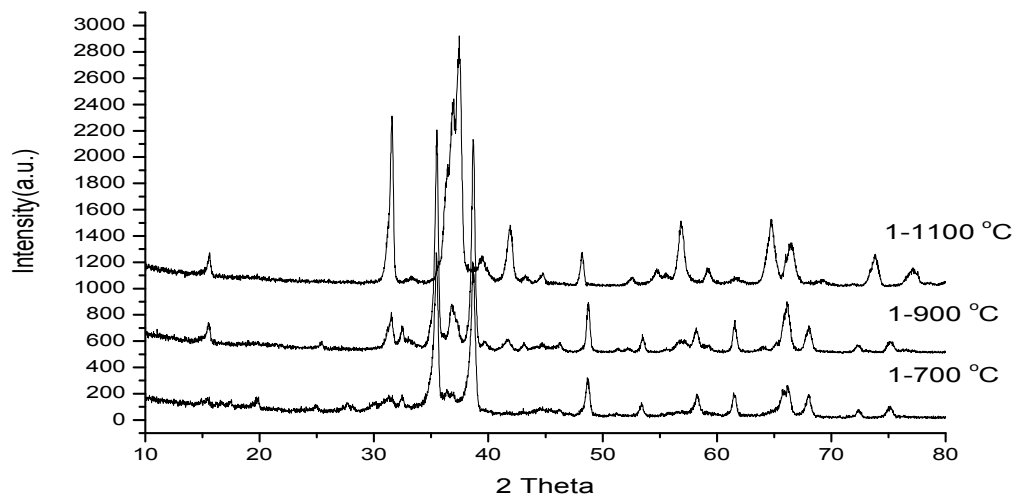


Fig.8: X-ray diffraction pattern of the pigment sample (1)

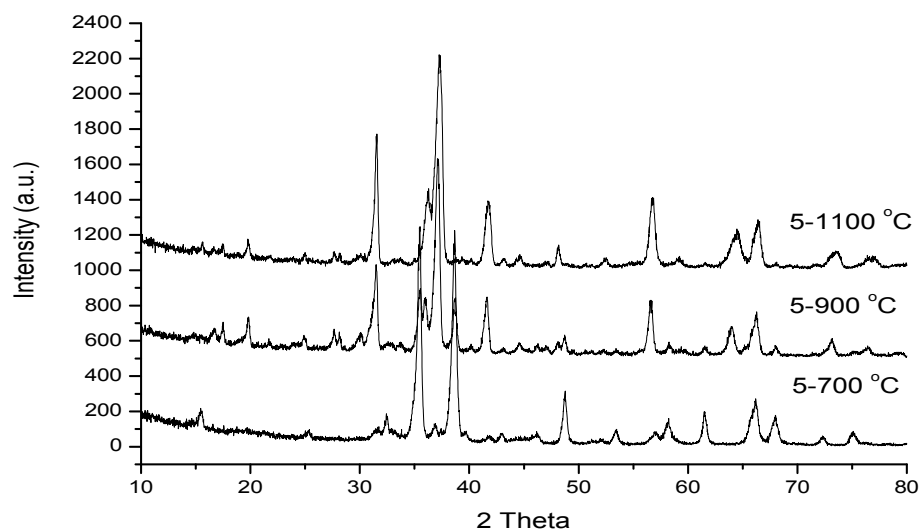


Fig.9: X-ray diffraction pattern of the pigment sample (5)

The X-rays diffraction for cobalt and chromium ion as doping for $MgAl_2O_4$ system using urea and glucose as fuel is investigated as powders at different calcinations temperatures. Fig () shows the XRD patterns of the samples fired at 500 °C, 700 °C, 900 °C and 1100 °C for 1 h, respectively. The sample fired at 500 at 500 was dark brown in colour and showed crystal phases of oxides. From X-ray patterns, it is clear that the intensity of the bands is increasing with calcined temperatures. The calcinated powders begin to form the spinel crystalline and the disappearance of Al_2O_3 at 900 °C. With the increase of the temperature above 900, in tensities of the peaks increase gradually until sharpen peaks are observed at 1100 °C. The samples fired at 700, 900 and 1100 °C were black in colour. The spinel was obtained for sample fired at 1100 °C.

The particle size of the samples fired at 1100°C were calculated according to Scherrer formula

$$d = k \lambda / B \cos \theta$$

Where d is the particle size, λ is the wavelength of the X-ray, $\lambda = 0.15317 \text{ nm}$, θ is Bragg angle, B is half height width of diffraction peak, $k = 0.9$. The crystalline diameters were calculated on each diffraction peak for the sample fired at 1100 °C and the average crystallite diameter was about 30 nm. Some peaks attributed to Cr^{3+} were found because of its height amount.

3.4. Colored Measurements

The CIE L^* a^* b^* colour parameters of powder samples and optimum parameters obtained in the optimization of ceramics samples are shown in Table (5). The samples 1 to 5 are best black coloured because minimize L^* a^* b^* parameters among all samples,

included the ceramic optimized samples. Sample 1 present also a good black colour. In order to minimize the presence of undesired environmental components in the system, sample 5 have high percent of Cr and result in good black pigment. On the other hand sample 1 gives the best black colored sample minimizing Cr presence substituted by Al in the composition. All good coloured black powders present spinel as only XRD detected crystalline phase (Table 5).

Table 5: CIE L^* a^* b^* parameter of colour samples

samples	L^*	a^*	b^*
1-700	40.2	1.5	1.3
1-900	41.4	1.7	1.7
1-1100	40.3	0.4	0.2
5-700	41.1	1.4	1.1
5-900	42.0	1.9	2.0
5-1100	40.2	0.5	0.3

3.5. Scanning Electron Microscope

The studies of micrographs of the calcites powders have revealed that crystallization of the powder begins above 700 °C and at 1100 °C the spinel crystallize completely with an average crystalline size of the order 0.8- 2.0 μm . Figure () shows a micrograph for a $CoCr_2O_4$ powder heat treated at 900 C and Figure (b) at 1100 C. At 900 the spinel phases start to crystallize and at 1100 C the phase is totally formed. The mean particle size ranges from 0.8 to 1.0 μm are formed. This pigment displays a grain morphology consisting of perfect octahedrons characteristic of spinels.

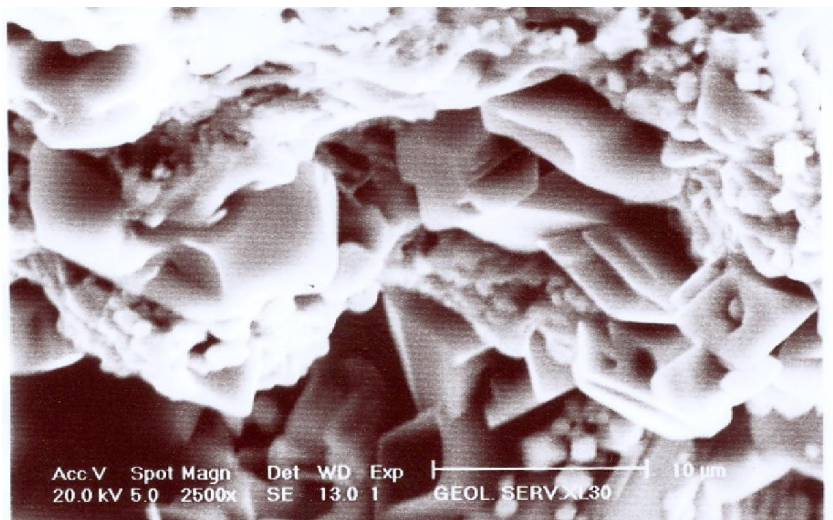


Fig.10: SEM micrographs of black pigments sample 1 at 1100 °C

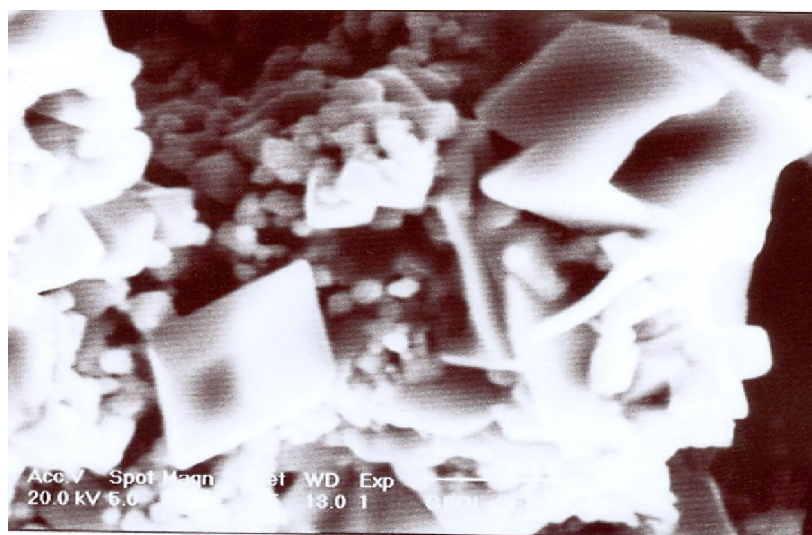


Fig.11: SEM micrographs of black pigments sample 5 at 1100 °C

Conclusion

This study represents one of the methods to prepare color spinel as combustion reaction

1- this paper has been the study of the mode of decomposition of coordinated D-glucose/urea in presence of chromium(III)/cobalt(II) or aluminum(III)/cobalt(II) complex systems in dry grinding at room and high temperatures.

2- The present investigation was undertaken to study the nature of the reaction of urea with metal ions at room temperature. Furthermore, the role played by certain metal ions such as Cr^{3+} , Al^{3+} , and Co^{2+} on the decomposition of coordinated urea and D-glucose is of considerable interest

3- The infrared spectra of both parent adducts of urea and D-glucose with Cr(III)/Co(II) and Al(III)/Co(II) (Fig. 2, Table 3) and they indicated that, oxygen-to-metal bonds are present in these adducts

4- The thermal degradation of the Cr (III)/Co (II) and Al (III)/Co (II) systems ignited previously at ~ 300 °C take place in three degradation stages.

5- These stages of degradation at 179 °C are accompanied by weight of loss 5.00% corresponding to the loss of carbon dioxide molecules.

6- The mass loss of the second thermal decomposition step of glucose or urea

7- Thermal behaviors of the Cr (III)/Co (II) and Al (III)/Co (II) systems ignited previously at ~ 300 °C

in terms of stability ranges, peak temperatures and values of kinetic parameters are discussed.

8- The thermograms and the calculated thermal parameters for the systems show that the stability of these adducts depends on the nature of the central metal ion. The thermal stability of the metal complexes was found to increase periodically with increase in atomic number of the metal and the larger value of charge/radius ratio

9- The calcinated powders begin to form the spinel crystalline and the disappearance of Al_2O_3 at 900°C

10- The samples fired at 700 , 900 and 1100°C were black in colour.

11- The average crystallite diameter was about 30 nm . Some peaks attributed to Cr^{3+} were found because of its height amount

12- Sample 1 present also a good black colour. The sample 5 has high percent of Cr and result in good black pigment.

13- The sample 1 gives the best black colored sample minimizing Cr presence substituted by Al in the composition.

14- The spinel crystallizes completely with an average crystalline size of the order $0.8\text{--}2.0\ \mu\text{m}$.

15- This pigment displays a grain morphology consisting of perfect octahedrons characteristic of spinels.

References

- I. Ganesh, B. Srinivas, R. Johnson, B. P. Saha, and Y. R. Mahajan, *Br. Ceram. Trans.*, 2002, **101**, 247–254.
- I. Ganesh, R. Johnson, G. V. N. Rao, Y. R. Mahajan, S. S. Madavendra, and B. M. Reddy, *Ceram. Int.*, 2005, **31**, 67–74.
- A. K. Adak, S. K. Saha, and P. Pramanik, *J. Mater. Sci. Lett.*, 1997, **16**, 234–235.
- J. G. Li, T. Ikegami, J. H. Lee, and T. Mori, *J. Am. Ceram. Soc.*, 2000, **83**, 2866–2868.
- N. Yang, and L. Chang, *Mater. Lett.*, 1992, **15**, 84–88.
- S. K. Behera, P. Barpanda, S. K. Pratihari, and S. Bhattacharyya, *Mater. Lett.*, 2004, **58**, 1451–1455.
- H. Zhang, X. Jia, Z. Liu, and Z. Li, *Mater. Lett.*, 2004, **58**, 1625–1628.
- J. C. Debsikdar, *J. Mater. Sci.*, 1985, **20**, 4454–4458.
- M. K. Naskar, and M. Chatterjee, *J. Am. Ceram. Soc.*, 2005, **88**, 38–44.
- J. Guo, H. Lou, H. Zhao, X. Wang, and X. Zheng, *Mater. Lett.*, 2004, **58**, 1920–1923.
- P. A. Lewis, *Pigment Handbook*, Vol. 1. John Wiley and Sons, New York, 1998.
- C. Otero Area, M. Pen˜ arroya Mentrui, E. Escalona Platero, F. X. Llabre˜ s i Xamena, and J. B. Parra, *Mater. Lett.*, 1999, **39**, 22–27.
- Sesiroˆ , ITOˆ , Tadahiro, Oˆ kawa and Tosihide, Kuwahara, *J. Jpn. Soc. Color Mat.*, 1981, **54**, 339–343 (Japanese).
- Japanese Patent, 4-55322, 1992.
- Japanese Patent, 4-55323, 1992.
- Japanese Patent, 2-283771, 1990.
- S. Chemlala, A. Larbotb, M. Persinb, J. Sarrazinb, M. Sghyara, and M. Rafiqqa, *Mater. Res. Bull.*, 2000, **35**, 2515–2523.
- W. S. Cho, and M. Kakihana, *J. Alloys and Compounds*, 1999, **287**, 87–90.
- J. J. Kingsley and K. C. Patil, *Mater. Lett.*, 1988, **6**, 427–432.
- J. J. Kingsley, K. Suresh and K. C. Patil, *J. Mater. Sci.*, 1990, **25**, 1305–1312.
- D. A. Fumo, M. R. Morelli and A. M. Segada˜ es, *Mater. Res. Bull.*, 1996, **31**, 1243–1255.
- J. D. Cunha, D. M. A. Melo, A. E. Martinelli, M. A. F. Melo, I. Maia, S. D. Cunha, *Dyes Pigments* **65** (2005) 11.
- C. C. Hwang, T. Wu. Yung, J. Wan, J. S. Tsai, *J. Mater. Sci. Eng. B* **111** (2004) 49.
- S. Ekambaram, *J. Alloys Compd.* **390** (2005) 14.
- P. Duran, J. Tartaj, F. Rubio, C. Moure, O. Pena, *J. Ceram. Int.* **31** (2005) 599.
- P. Barpanda, S. K. Behera, P. K. Gupta, S. K. Pratihari and S. Bhattacharya, *J. Eur. Ceram. Soc.* **26** (2006) 2603.
- S. Cavaa, S. M. Tebcherani, S. A. Pianaro, C. A. Paskocimas, E. Longo, J. A. Varela, *Mater. Chem. Phys.* **97** (2006) 102.
- F. Bondioli, T. Manfredini, M. Romagnoli, *J. Eur. Ceram. Soc.* **26** (2006) 311.
- V. Koleva, D. Mehandjiev, *Mater. Res. Bull.* **41**, **3**, 469 (2006).
- V. Koleva, H. Effenberger, *J. Solid State Chem.* **180** (2007) 956.
- B. Boonchom, C. Danvirutai, *Ind. Eng. Chem. Res.* **46**, 9071 (2007).
- T. Singanahally Aruna, S. Alexander Mukasyan, *Current Opinion in Solid State and Materials Science* **12** (2008) 44–50
- K. C. Patil, S. T. Aruna, T. Mimanim, *Combustion synthesis: an update. Curr Opin Solid State Mater Sci* **2002**; **6**: 507–12.
- R. E. Muenchausen, E. A. McKigney, J. Jacobsohn LG, Blair MW, Bennett BL, Cooke DW. *Science and application of oxyorthosilicate nanophosphors. IEEE Trans Nucle Sci* **2008**; **55**: 1532–5.
- H. Song, D. Chen, *Lumin* **2007**; **22**: 554–8.
- Z. Qiu, Y. Zhou, M. Lü, A. Zhang, Q. Ma, *Dy nanocrystals. Solid State Sci* **2008**; **10**: 629–33.

37. S. Ekambaram, *J Alloys Comp* 2005;390:L7–9.
38. Y. Jin, W.P. Qin, J.S. Zhang, Y. Wang, C.Y. Cao, *J Solid State Chem* 2008;181:724–9.
39. X.M. Lou, D.H. Chen. *Mater Lett* 2008; 62:1681–4.
40. Z. Qiu, Y. Zhou, M. Lu, A. Zhang, Q. Ma, *Acta Mater* 2007;55:2615–20.
41. R. Krsmanović, V.A. Morozov, O.I. Lebedev, S. Polizzi, A. Speghini, M. Bettinelli, et al. *Nanotech* 2007;18:325604–13.
42. L. Xu, B. Wei, Z. Zhang, Z. Lü, H. Gao, Y. Zhang. *Nanotech* 2006;17:4327–31.
43. T. Pine, X. Lu, R. Daniel, G. Mumm, and J. Scott Brouwer. *J Am Ceram Soc*, 2007;90:3735–40.
44. R. Ianos, I. Lazau, C. Pacurariu, P. Barvinschi, *Eur J Inorg Chem* 6;2008:925–30.
45. M. Edriss and R. Norouzbeigi, *Mater Sci Pol* 2007;25:1029–40.
46. J. Ma, C. Jiang, X. Zhou, G. Meng, X. Liu, *J Alloys Comp* 2008;455:364–8.
47. S. Vivekanandhan, M. Venkateswarulu, N. Satyanarayana, *Mater Chem Phys* 2008; 109:141–8.
48. S.T. Aruna, K.S. Rajam, *Mater Res Bull* 2004; 39:157–67.
49. S. Sasikumar, R. Vijayaraghavan, *Ceram Int* 2008; 34:1373–9.
50. P.S. Devi, S. Banerjee, *Ionics* 2008; 14:73–8.
51. R. Ianos, I. Lazau, C. Pacurariu, P. Barvinschi, *Eur J Inorg Chem* 2008;6:931–8.
52. M. Cain, R. Morrell, *Appl. Organomet. Chem.* 15 (2001) 321.
53. Z. Hu, M. Xue, Q. Zhang, Q. Sheng, Y. Liu, *Dyes Pigm.* 76 (2008) 173.
54. S.K. Biswas, D. Dhak, A. Pathak, P. Pramanik, *Mater. Res. Bull.* 43 (2008) 665.
55. G. Buxbaum, *Industrial Inorganic Pigments*, second ed., Wiley-VCH, 1997.
56. A. Burgyan, *Intereram. NR 1* (1979) 30.
57. E.S. Kharashvili, *Glass Ceram.* 42 (1985) 459.
58. R.W. Batchelor, *Trans. Br. Ceram. Soc.* 73 (1974) 297.
59. J. Livage, *Inorganic Materials, Sol–Gel Synthesis of*, *Encyclopedia of Materials: Science and Technology*, 2010, ISBN 0-08-0431526, pp. 4105–4108.
60. D. Segal, *J. Mater. Chem.* 7 (1997) 1297.
61. C.O. Arean, M.P. Mentruit, E.E. Scalona, F.X. Xamena, J.B. Parra, *Mater. Lett.* 12 (1999) 537.
62. P. Phule, T.E. Wood, *Sol–Gel Synthesis of Ceramics and Glasses*, *Encyclopedia of Materials: Science and Technology*, 2004, ISBN 0-08-0431526, pp. 1090–1095.
63. M. Iade H. Mays, J. Schmidt, R. Willumeit, R. Schomacker, *Colloids Surfaces A: Physicochem.* 163 (2000) 3.
64. R.E. Riman, W.L. Suchanek, M.M. Lencka, *Ann. Chim. Sci. Mater.* 27 (2002) 15.
65. Z. Chen, E. Shi, W. Li, Y. Zheng, N. Wu, W. Zhong, *J. Am. Ceram. Soc.* 85 (2002) 2949.
66. Y.W. Chen, T.M. Yen, C. Li, *J. Non-Cryst. Solids* 185 (1995) 49.
67. R. Julian, J. Osman, J.A. Crayston, A. Pratt, D.T. Richens, *Mater. Chem. Phys.* 110 (2008) 256.
68. K. Kim, C. Kim, *J. Eur. Ceram. Soc.* 24 (2004) 2613.
69. M. Kakihana, *J. Sol–Gel Sci. Technol.* 6 (1996) 7.
70. X. Yu, X. He, S. Yang, X. Yang, X. Xu, *J. Mater. Lett.* 58 (2003) 48.
71. I.S. Ahmed, H.A. Dessouki, A.A. Ali, *Spectrochim. Acta* 71A (2008) 616.
72. I.S. Ahmed, H.A. Dessouki, S.A. Shama, M.M. Moustafa, A.A. Ali, *Spectrochim. Acta* 74A (2009) 665.
73. R. Ianos, I. Lazau, C. Pacurariu, P. Barvinschi, *Mater. Res. Bull.* 43 (2008) 3408.
74. X. Huang, J. Chang, *Mater. Chem. Phys.* 115 (2009) 1.
75. M.D. Nersesyan, A.G. Peresada, A.G. Merzhanov, *Int. J. SHS* 7 (1998) 60.
76. R. Ianos, I. Lazau, *Mater. Chem. Phys.* 115 (2009) 645.
77. P. Barpanda, S.K. Behera, P.K. Gupta, S.K. Pratihari, S. Bhattacharya, *J. Eur. Ceram. Soc.* 26 (2006) 2603.
78. S.T. Aruna, S. Ghosh, K.C. Patil, *Int. J. Inorg. Mater.* 3 (2001) 387.
79. D.S. Gouveia, L.E.B. Soledade, C.A. Paskocimas, E. Longo, A.G. Souza, I.M.G. Santos, *Mater. Res. Bull.* 41 (2006) 2049.
80. R.A. Candeia, M.A.F. Souza, M.I.B. Bernardi, S.C. Maestrelli, *Mater. Res. Bull.* 41 (2006) 183.
81. R.A. Candeia, M.A.F. Souza, M.I.B. Bernardi, S.C. Maestrelli, I.M.G. Santos, A.G. Souza, E. Longo, *Ceram. Int.* 33 (2007) 521.
82. R.A. Candeia, M.I.B. Bernardi, E. Longo, I.M.G. Santos, A.G. Souza, *Mater. Lett.* 58 (2004) 569.
83. R.K. Mason, *J. Am. Ceram. Soc. Bull.* 40 (1961) 5.
84. G. Monnari, T. Manfredi, *J. Ceram. Eng. Sci. Process* 17 (1996) 102.
85. V. Sepelak, K.D. Becker, *Mater. Sci. Eng. A* 375–377 (2004) 861.
86. M. Llusar, A. Forés, J.A. Badenes, J. Calbo, M.A. Tena, G. Monrós, *J. Eur. Ceram. Soc.* 21 (2001) 1121.
87. W. Li, J. Guo, J. Li, *J. Eur. Ceram. Soc.* 23 (2003) 2289.
88. D.V. Sanghani, G.R. Abrams, P.J. Smith, *Trans. J. Br. Ceram. Soc.* 80 (1981) 210.

90. S.C. Lee and H.O. Lintang, L. Yuliati, *Chem Asian J.*, 7(9) (2012) 2139.
91. M. Zhang, J.-J. Lv, F.-F. Li, N. Bao, A.-J. Wang, J.-J. Feng and D.-L. Zhou, *Electrochimica Acta*, 123 (2014) 227.
92. A. Chu, M. Qin, D. Li, H. Wu, Z. Cao and X. Qu, *Materials Chem. Physics*, 144(3) (2014) 560.
93. A. Yamaguchi, T. Miyazawa, T. Shimanouchi and S. Mizushima, *Spectrochim. Acta*, 10 (1957) 170.
94. J. E. Stewart, *J. Chem. Phys.*, 26 (1957) 248.
95. R.B. Penland, S. Mizushima, C. Curran and J.V. Quagliano, *J. Amer. Chem. Soc.*, 79 (1957) 1575.
96. G. Cerchiaro, A.C. Sant'Ana, M.L. Temperini and A.M. da Costa Ferreira, *Carbohydr Res.*, 340(15) (2005) 2352.
97. I.R. Beattie, T.R. Gilson and G.A. Ozin, *J. Chem. Soc. (A)*, (1969) 534.
98. Colthup, *J. Opt. Soc. Amer.*, 40 (1950) 397.
99. T.S. Shevchuk, A.F. Borina and V.V. Volkov, *Zh. Neorg. Khim.*, 37(6) (1992) 1355.
100. A.F. Borina, V.T. Orlova and S.A. Popova, *Zh. Neorg. Khim.*, 36(10) (1991) 2617.
101. N.G. Furmanova, D.K. Sulaimankulova, V.F. Resnyanskii and K.S. Sulaimankulov, *Kristallografiya*, 41(4) (1996) 669.
102. A. Kozak, K. Wieczorek-Ciurowa and K. Pielichowski, *J. Therm. Anal.*, 45(5) (1995) 1245.
103. E.M. Nour, S.M. Teleb, N.A. Al-Khsosy and M.S. Refat, *Synth. React. Inorg. Met.-Org. Chem.*, 27(4) (1997) 505.
104. M.S. Refat, S.M. Teleb and S.A. Sadeek, *Spectrochim. Acta Part A*, 60(12) (2004) 2803.
105. Vogel, "Qualitative Inorganic Analysis", John Wiley & Sons, Inc. New York, (1987).
106. E.S. Freeman and B. Carroll, *J. Phys. Chem.*, 62 (1958) 394.
107. A.W. Coats and J.P. Redfern, *Nature*, 201 (1964) 68.
108. H.W. Horowitz and G. Metzger, *Anal. Chem.*, 35 (1963) 1464.
109. J.H.F. Flynn, and L.A. Wall, *J. Res. Natl. Bur. Stand.*, 70A (1966) 487.
110. W. Malik, G.D. Tuli and R.D. Madan, Selected topics in inorganic chemistry, New Delhi: Chand and Co. Ltd., 1984.

3/11/2014